Physics Letters B 780 (2018) 325–331

Contents lists available at ScienceDirect

Physics Letters B

www.elsevier.com/locate/physletb

Interplay of quasiparticle-vibration coupling and pairing correlations on β-decay half-lives

Y.F. Niu [a,*], Z.M. Niu [b], G. Colò [c,d], E. Vigezzi [d]

[a] ELI-NP, "Horia Hulubei" National Institute for Physics and Nuclear Engineering, 30 Reactorului Street, RO-077125, Bucharest-Magurele, Romania
[b] School of Physics and Material Science, Anhui University, Hefei 230601, China
[c] Dipartimento di Fisica, Università degli Studi di Milano, via Celoria 16, I-20133 Milano, Italy
[d] INFN, Sezione di Milano, via Celoria 16, I-20133 Milano, Italy

ARTICLE INFO

Article history:
Received 1 November 2017
Received in revised form 24 January 2018
Accepted 26 February 2018
Available online 28 February 2018
Editor: J.-P. Blaizot

Keywords:
β-decay
Quasiparticle random phase approximation
Quasiparticle vibration coupling
Isoscalar pairing

ABSTRACT

The nuclear β-decay half-lives of Ni and Sn isotopes, around the closed shell nuclei ^{78}Ni and ^{132}Sn, are investigated by computing the distribution of the Gamow–Teller strength using the Quasiparticle Random Phase Approximation (QRPA) with quasiparticle-vibration coupling (QPVC), based on ground-state properties obtained by Hartree–Fock–Bogoliubov (HFB) calculations. We employ the effective interaction SkM* and a zero-range effective pairing force. The half-lives are strongly reduced by including the QPVC. We study in detail the effects of isovector (IV) and isoscalar (IS) pairing. Increasing the IV strength tends to increase the lifetime for nuclei in the proximity of, but lighter than, the closed-shell ones in QRPA calculations, while the effect is significantly reduced by taking into account the QPVC. On the contrary, the IS pairing mainly plays a role for nuclei after the shell closure. Increasing its strength decreases the half-lives, and the effect at QRPA and QRPA+QPVC level is comparable. The effect of IS pairing is particularly pronounced in the case of the Sn isotopes, where it turns out to be instrumental to obtain good agreement with experimental data.

1. Introduction

The nuclear β-decay is an important weak-interaction process, which not only provides information on spin and isospin properties of the nuclear effective interaction, but also sets the time scale of the rapid neutron-capture process (r-process), and hence determines the production of heavy elements in the universe [1–3]. Moreover, in particle physics β-decay has provided the first experimental evidence of parity violation [4] and can be employed to verify the unitarity of the CKM matrix [5,6].

Important advances in the measurement of β-decay half-lives have been achieved in recent years with the development of radioactive ion-beam facilities. For example, the β-decay half-lives of 38 neutron-rich isotopes from $_{36}$Kr to $_{43}$Tc with neutron number between 50 and 82 [7], of 20 neutron-rich nuclei with $Z = 27 - 30$ in the ^{78}Ni region [8], of 110 neutron-rich isotopes of elements between $_{37}$Rb and $_{50}$Sn (across the $N = 82$ shell gap) [9], and of 94 neutron-rich isotopes between $_{55}$Cs and $_{67}$Ho [10], were measured at RIKEN. The newly obtained experimental data provide an optimal testground for theoretical models. The r-process nuclei at the $N = 126$ shell closure are, instead, still not experimentally reachable; thus, accurate theoretical models for half-life calculations are crucial for the study of the r-process nucleosynthesis.

QRPA is one of the most commonly used models for the calculation of the β-decay half-lives. Many versions of QRPA have been implemented to this aim, from models that are based at least in part on phenomenological ingredients [11–15] to self-consistent models without adjustable parameters based on both nonrelativistic [16–21] and relativistic Energy Density Functionals (EDFs) [22–31]. In the QRPA calculations, the half-lives are usually overestimated; the remedy often consists in tuning up the strength of an attractive isoscalar (IS) proton–neutron (pn) pairing force which is introduced in QRPA and does not affect ground-state properties [14,16,26–29]. However, the isoscalar pn pairing has no, or little, effect on closed-shell nuclei like ^{78}Ni and ^{132}Sn as well as on the nuclei before the shell closure [16,26–29]. Therefore, there must exist other correlations than isoscalar pn pairing, that are capable to reduce such half-lives. One possible candidate is an attractive tensor force as it has been pointed out in Refs. [32,33]. Also this requires the introduction of new terms in the Hamiltonian and the tuning of one or more parameters.

* Corresponding author.
E-mail address: yifei.niu@eli-np.ro (Y.F. Niu).

https://doi.org/10.1016/j.physletb.2018.02.061

Another possible solution is the inclusion of new correlations beyond QRPA without introducing new parameters. This is particularly evident in the case of magic nuclei, in which QRPA becomes simple RPA. The RPA approach is restricted to configurations of one particle–one hole (1p–1h) nature. It is well known that this is not sufficient for the description of the spreading width of giant resonances. In order to reproduce the observed widths, one must consider the damping caused by the coupling to more complicated states, like 2p–2h configurations [34–38]. An effective way to account for (most of) the observed spreading widths is to take into account the coupling of single-nucleon states to the collective low-lying (mainly surface) nuclear vibrations or phonons (that is, to include 1p–1h–1 phonon configurations in the model space) [39]. We call this model RPA plus PVC, and we note that self-consistent versions of such a model have been realized based on both relativistic and nonrelativistic energy functionals. Good agreement with the experiment has been obtained for the line shape of the Gamow–Teller (GT) and spin-dipole strength distribution [40–43]. In our application of the RPA+PVC model, based on Skyrme energy density functionals [42,43], it has been found that the coupling to phonons produces a downward shift of the GT strength, accompanied by the development of broadening and/or fragmentation.

Since β-decay is dominated by the low-lying GT transitions below the Q_β value, it is expected that the effect of PVC on the GT excitations can help in reducing the half-lives. To demonstrate the effect of PVC on half-lives, we have applied our self-consistent Skyrme RPA+PVC model to magic nuclei, and have shown that the inclusion of PVC considerably improves the agreement of β-decay half-lives with experiment [44]. However, the above investigation was limited to magic nuclei since pairing correlations were not included. Recently, the self-consistent QRPA with quasiparticle-vibration coupling (QRPA+QPVC) model, based either on Skyrme EDFs [45] or on relativistic EDFs [46], was developed and used to study the GT transitions in superfluid nuclei. This new development opens up the possibility to explore the β-decay half-lives for a whole isotopic chain. In Ref. [46], the half-lives of Ni isotopes were investigated by means of the QRPA+QPVC model based on the relativistic EDFs, and it was found that the inclusion of QPVC can reduce the half-lives. However, isoscalar pairing was not included in the calculations.

In this Letter, we are going to use the self-consistent QRPA+QPVC model based on the Skyrme EDFs, with the inclusion of isoscalar pairing, to investigate the half-lives of Ni and Sn isotopes. Since Ni and Sn isotopes have a magic number of protons, they will be considered as spherical in our calculations. In particular, the effects of isovector pairing and isoscalar pairing, as well as their interplay with effects related to QPVC, are explored in detail. The comparison of the theoretical results with experimental data can give relevant indications on the value of the isoscalar pairing strength, which is still under active discussion. Several pieces of information, that have been reviewed in [47], point to a value of the IS pairing strength of the order of 1.5 that of the IV pairing. Further independent confirmations of this finding would be very valuable.

2. Formalism

We first carry out a self-consistent HFB+QRPA calculation of the GT strength, using the SkM* effective interaction. We choose the interaction SkM* because it gives a good description of GT resonances in magic and superfluid nuclei and β-decay half-lives in magic nuclei at the (Q)PVC level, consistently improving the results obtained in QRPA, as shown in previous studies [42–45]. The detailed formulas of charge-exchange QRPA on top of HFB can be found in Ref. [48]. In our formalism, only the IV $T = 1$ pairing correlations are taken into account to describe the ground-state. Since we do not consider nuclei close to $N = Z$ this should be a reasonable approximation. Pairing must be included also in the residual QRPA force, and for a zero-range force only its $T = 0$ component plays a role for the GT excitations. We adopt a density-dependent, zero-range, surface pairing force which is parameterized as follows [48]:

$$V_{T=1}(\mathbf{r}_1, \mathbf{r}_2) = f_{iv} V_0 \frac{1 - P_\sigma}{2}(1 - \frac{\rho(\mathbf{r})}{\rho_0})\delta(\mathbf{r}_1 - \mathbf{r}_2), \tag{1}$$

$$V_{T=0}(\mathbf{r}_1, \mathbf{r}_2) = f_{is} V_0 \frac{1 + P_\sigma}{2}(1 - \frac{\rho(\mathbf{r})}{\rho_0})\delta(\mathbf{r}_1 - \mathbf{r}_2), \tag{2}$$

where $\mathbf{r} = (\mathbf{r}_1 + \mathbf{r}_2)/2$, ρ_0 is taken to be 0.16 fm^{-3}, and P_σ is the spin exchange operator.

The QRPA in its standard matrix form produces a set of 1^+ eigenstates $|n\rangle$ with forward-going and backward-going amplitudes denoted by $X^{(n)}_{ab}$ and $Y^{(n)}_{ab}$, having energies E_n and associated values of the B(GT) strength B_n. We then couple these QRPA states with a set of doorway states consisting of a two-quasiparticle excitation coupled to a collective vibration. The properties of these collective vibrations, i.e. phonons $|nL\rangle$, are, in turn, obtained by computing the QRPA response with the same Skyrme interaction, for states of natural parity $L^\pi = 0^+$, 1^-, 2^+, 3^-, 4^+, 5^-, and 6^+. The phonons are built out of proton–proton or neutron–neutron excitations, so only the IV pairing is included in the residual interaction entering the QRPA calculation. We have retained in our model space the phonons with energy less than 20 MeV and absorbing a fraction of the non-energy weighted isoscalar or isovector sum rule (NEWSR) strength larger than 5%.

The self-energy of the QRPA state $|n\rangle$ is given by

$$\Sigma_n(E_M) = \sum_{ab,a'b'} W^{\downarrow}_{ab,a'b'}(E_M) X^{(n)}_{ab} X^{(n)}_{a'b'} + W^{\downarrow *}_{ab,a'b'}(-E_M) Y^{(n)}_{ab} Y^{(n)}_{a'b'}, \tag{3}$$

where the matrix elements $W^{\downarrow}_{ab,a'b'}(E_M)$ are spreading terms associated with the coupling of two-quasiparticle configurations with the doorway states, and defined in Ref. [45]. They are complex and energy-dependent, and they must be calculated by using an averaging parameter η that avoids divergences and represents, in an approximate way, the coupling of the doorway states to even more complicated configurations. We have found that the lifetimes converge for small values of η, which are expected to be appropriate for low-lying, discrete states. In our calculations we have set $\eta = 200$ keV. One can then calculate the GT strength distribution from the Gaussian averaging [49],

$$S(E_M) = \sum_n \frac{1}{\sigma_n \sqrt{2\pi}} \mathrm{e}^{-\frac{(E_M - E_n - \Delta E_n)^2}{2\sigma_n^2}} B_n, \tag{4}$$

where σ_n is defined as $\sigma_n = (\frac{\Gamma_n}{2} + \eta)/\sqrt{2\ln 2}$, with $\Delta E_n = \mathrm{Re}\Sigma_n(E_M)$ and $\Gamma_n = -2\mathrm{Im}\Sigma_n(E_M)$.

Once the strength function has been obtained, the β-decay half-life of an even–even nucleus is calculated in the allowed GT approximation by using the expression [16,29,44,50]

$$T_{1/2} = \frac{D}{g_A^2 \int^{Q_\beta} S(E) f(Z, \omega) dE}, \tag{5}$$

where $D = 6163.4$ s, and we set g_A equal to 1 rather than to its free value of 1.26, to account for the quenching of isovector spin

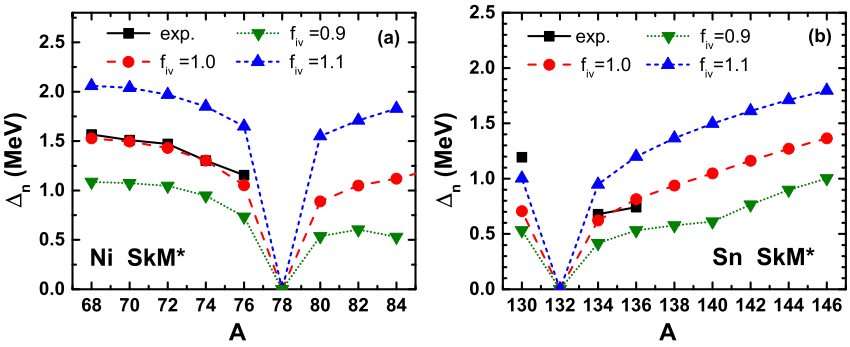

Fig. 1. (Colour online.) Neutron pairing gaps of Ni (left panel) and Sn (right panel) isotopes. They are calculated with different isovector pairing strength, and compared with the experimental values obtained from the three point formula (see the text).

matrix elements [51,16], as is commonly done in QRPA calculations [16,15,18–20,28,29]. Notice that here the energy E refers to the ground state of the daughter nucleus, which is related to the energy E_M referred to the ground state of the mother nucleus by $E = E_M - \Delta B$, ΔB being the experimental binding energy difference $B_M - B_D$. The integrated phase volume $f(Z,\omega)$ is given by

$$f(Z,\omega) = \int_{m_e c^2}^{\omega} p_e E_e (\omega - E_e)^2 F_0(Z+1, E_e) dE_e, \qquad (6)$$

where p_e, E_e, and $F_0(Z+1, E_e)$ denote the momentum, energy and Fermi function of the emitted electron, respectively. ω is the energy difference between the initial and final nuclear state, connected with the GT energy E (or E_M) by $\omega = Q_\beta + m_e c^2 - E = \Delta_{np} - E_M$ (where $\Delta_{np} = 1.293$ MeV is the mass difference between neutron and proton).

3. Results and discussions

Fig. 1 shows the HFB neutron pairing gaps of Ni and Sn isotopes. We include quasiparticles up to a maximum angular momentum $J_{\max} = 15/2$, and up to a maximum energy of 100 MeV. The strength of isovector ($T = 1$) pairing is adjusted to reproduce the empirical values of the pairing gaps (squares in Fig. 1), that are obtained from the experimental odd–even mass differences according to the 3-point formula $\Delta_n = -(-1)^N \frac{1}{2}[B(N-1,Z) + B(N+1,Z) - 2B(N,Z)]$, where B denotes the binding energy of the nucleus. As a result, we adopt the pairing strength parameter values $V_0 = -457$ and $V_0 = -520$ MeV fm^3, for Ni and Sn isotopes respectively. In order to study the effect of isovector pairing on the β-decay half-lives, we vary these pairing strength parameters by $\pm 10\%$, i.e., we change f_{iv} from 0.9 to 1.1 (see Eq. (1)). The resulting pairing gaps vary by about $\pm 35\%$ and are shown in Fig. 1.

3.1. Isovector pairing

In Fig. 2, the β-decay half-lives of Ni and Sn isotopes, calculated either without pairing correlations ($f_{iv} = 0.0$) or with different isovector pairing strengths, are compared with the experimental data. In panels (a) and (c), the half-lives are calculated at the QRPA level, while in panel (b) and (d) they are calculated within the QRPA+QPVC model. So far, isoscalar pairing correlations are not included ($f_{is} = 0.0$). The first general observation is that the influence of IV pairing correlations is small, compared to the effects of QPVC. Looking in more detail at the results, one notices that the effect of f_{iv} is negligible for the isotopes close to, and especially beyond, the magic nuclei ^{78}Ni and ^{132}Sn (notice that contrary to experiment, the isotopes $^{130-134}$Sn are predicted to be stable in QRPA and then do not appear in Fig. 2(a)). In the case of Ni isotopes, the effect of f_{iv} increases progressively going from ^{78}Ni towards ^{68}Ni, that is, towards the middle of the shell where Δ_n is maximum (see Fig. 1). Larger values of f_{iv} lead to longer lifetimes. In the case of Sn isotopes, the lifetimes of $^{140-146}$Sn instead first decrease when pairing IV correlations are switched on going from $f_{iv} = 0$ to $f_{iv} = 0.9$, and then increase going to $f_{iv} = 1.1$.

This behaviour can be understood considering that pairing correlations have two competing effects on lifetime. On the one hand, a larger value of f_{iv} leads to a larger pairing gap and then to larger GT excitation energies, which in turn reduces the β-decay phase space and increases the lifetime. On the other hand, pairing correlations modify the occupation of single-particle levels and in some cases induce new low-energy transitions that tend instead to reduce the lifetime. In order to have a more microscopic understanding of the dependence of the lifetime on f_{iv} for the nuclei shown in Fig. 2, we plot the single-particle spectra of ^{80}Ni and ^{134}Sn in Fig. 3. Let us consider Ni isotopes first. Going from ^{68}Ni to ^{78}Ni the $1\nu g_{9/2}$ level is being filled; pairing correlations slightly modify the occupation factors and do not lead to new transitions. The most important transition determining the lifetime is $\nu 2p_{1/2} \to \pi 2p_{3/2}$. In the presence of pairing correlations, the energy of the corresponding 2qp excitation is increased and the lifetime becomes longer for increasing values of f_{iv}. This transition remains the dominant one also in the case of $^{80-84}$Ni, but is less influenced by pairing correlations due to the shift of the chemical potential to the shell above. As a consequence, the lifetime is insensitive to the value of f_{iv}. Turning now to Sn isotopes, the situation for $^{136-140}$Sn is qualitatively similar to the case of $^{80-84}$Ni. In this case the dominant transition is $\nu 2d_{3/2} \to \pi 2d_{5/2}$. Increasing the number of neutrons, the occupation of the orbital $\nu 1h_{9/2}$ becomes significant when pairing correlations are active, and in the case of $^{142-146}$Sn the dominant transition becomes $\nu 1h_{9/2} \to \pi 1h_{11/2}$. Opening new low-energy transitions by switching pairing on tends to reduce the lifetime; further increasing the value f_{iv} the competing effect on quasiparticle energies prevails and the lifetime increases, as was already noticed in Fig. 2(c).

The QRPA+QPVC results are shown in Fig. 2(b) and (d), again for different values of the isovector pairing strength. With the inclusion of QPVC, the half-lives are reduced systematically. The experimental half-lives of Ni isotopes are well reproduced, while the half-lives of Sn isotopes are still overestimated, although much less than before. We remind that no isoscalar pairing has been introduced so far. At the QPVC level, we find that the effect of isovector pairing is greatly reduced; we will discuss the underlying reason making reference to Fig. 4, in which ^{70}Ni has been picked up as an example.

In Fig. 4, the GT strength distributions (with respect to the daughter nucleus), the cumulative sums of the GT strengths, and

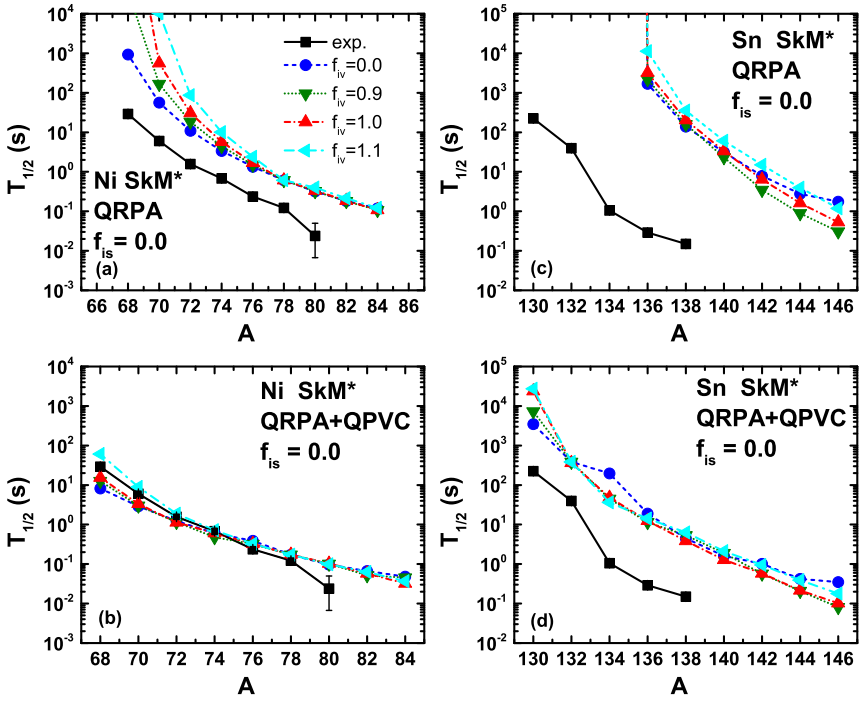

Fig. 2. (Colour online.) The β-decay half-lives of Ni [panel (a) and (b)] and Sn [panel (c) and (d)] isotopes calculated either by QRPA [panel (a) and (c)] or the QRPA+QPVC model [panel (b) and (d)], by using the Skyrme interaction SkM* with different IV pairing strengths for the ground state. The isoscalar pairing is not included in the calculations. The results are compared with the experimental data from Ref. [52].

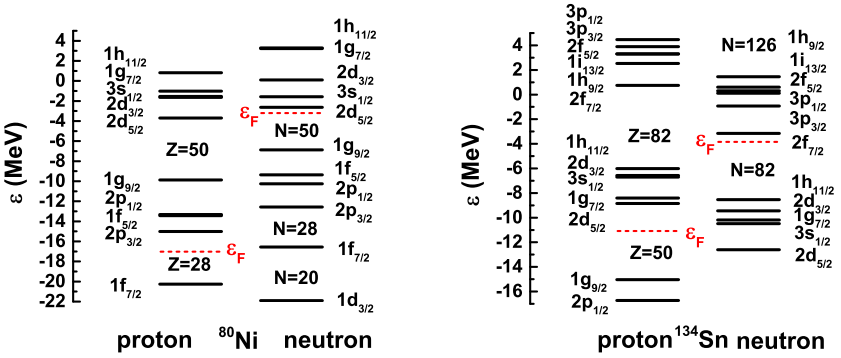

Fig. 3. (Colour online.) Neutron and proton single-particle spectra in ^{80}Ni and ^{134}Sn obtained by the diagonal matrix element of the HF field in canonical basis with the Skyrme interaction SkM*.

the cumulative sums of $1/T_{1/2}$ [that is, the values obtained from Eq. (5) when Q_β is replaced by a running E in the upper limit of the integral in the denominator] of ^{70}Ni are presented for different isovector pairing strengths ($f_{iv} = 0.0, 1.0$ and 1.1). In panel (a), the arrows indicate the experimental energies of the measured 1^+ states. At the QRPA level, one observes a single peak accompanied by a small strength at lower energy, which is only visible in panel (d) when multiplied by a factor of 10, in each case for $f_{iv} = 0, 1.0$ and 1.1. The QRPA excitation energy is increased as the pairing strength increases, which leads to an increase of the half-life, as discussed above. The QRPA excitation energy is much higher than the experimental 1^+ state energies, resulting in a strong overestimation of the experimental half-life (see Fig. 2(a)).

With the inclusion of QPVC, the QRPA peak is shifted downwards and some GT strength appears in the region of the experimental 1^+ states. The value of the shift is about 2 MeV for $f_{iv} = 0$ and about 2.8 MeV for $f_{iv} = 1.0$ and $f_{iv} = 1.1$ (cf. Figs. 4(a) and (d)). This difference is related to the fact that the collectivity of the 2^+ phonon and the associated QPVC vertex are much reduced in the absence of pairing correlations. The difference in the values of the energy shifts counterbalances the effect found at the QRPA level. As a consequence, the excitation energies and the lifetimes calculated with and without pairing turn out also to be similar (see Fig. 4(c) and Fig. 2(b)). Obviously, however, the experimental properties of low-lying collective phonons are much better described when pairing is included.

3.2. The role of isoscalar pairing

We investigate the role of isoscalar pairing in Fig. 5, where the β-decay half-lives of Ni and Sn isotopes, calculated by QRPA and QRPA+QPVC model without isoscalar pairing ($f_{is} = 0.0$) or with different isoscalar pairing strengths, are shown and compared with the experimental data. The strength of isovector pairing is fixed at $f_{iv} = 1.0$. IS pairing has almost no effect for nuclei with neutron number just before the shell closure (small effects are visible in Fig. 5 in the case of ^{68,70}Ni), but starts to play a role when neutron number goes across the shell closure, at both QRPA and

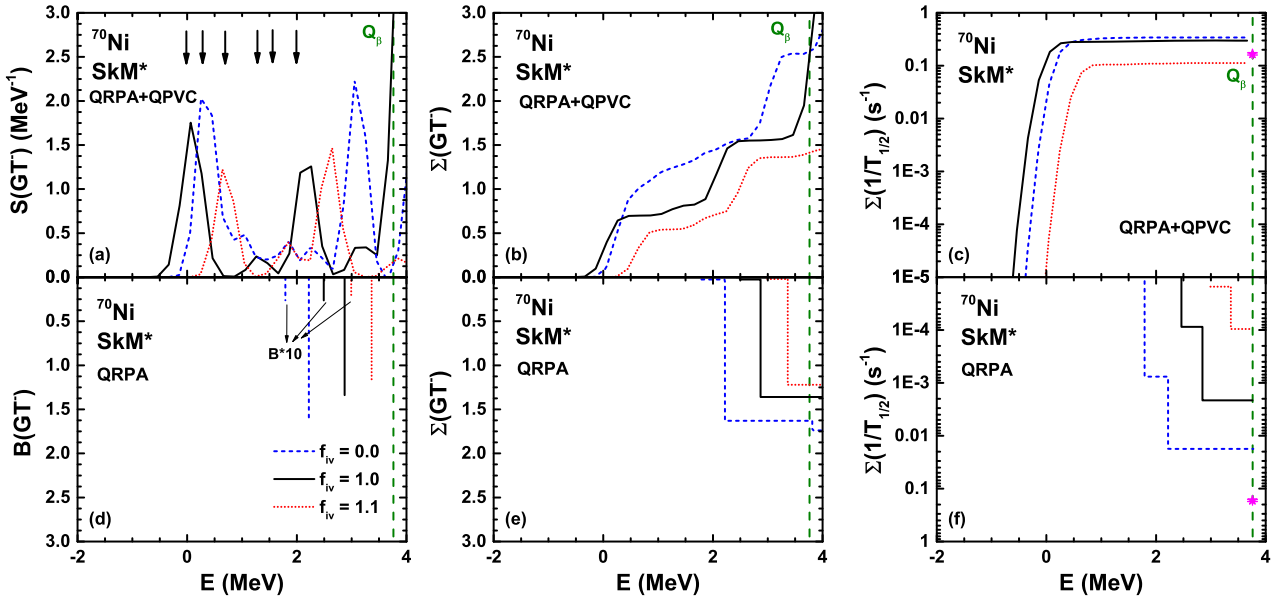

Fig. 4. (Colour online.) The GT strength distribution [panels (a) and (d)], the cumulative sum of GT strength [panels (b) and (e)], and the cumulative sum of $1/T_{1/2}$ [panels (c) and (f)] are displayed for the case of ^{70}Ni. The results are obtained by QRPA and QRPA+QPVC models, using the Skyrme interaction SkM* with different IV pairing strengths. Isoscalar pairing is not included in the calculations. In panel (a), the arrows indicate the experimental energies of the measured 1^+ states [53]. In panel (c) and (f), the experimental value of $1/T_{1/2}$ is indicated by the star [52]. In panel (d), the strengths indicated by arrows are multiplied by a factor of 10 to be visible. In these panels, the excitation energies calculated with respect to the mother nucleus are transformed to E, namely the excitation energies referred to the ground state of daughter nucleus, by using the experimental binding energy difference; accordingly, the vertical dashed lines show the experimental value of Q_β.

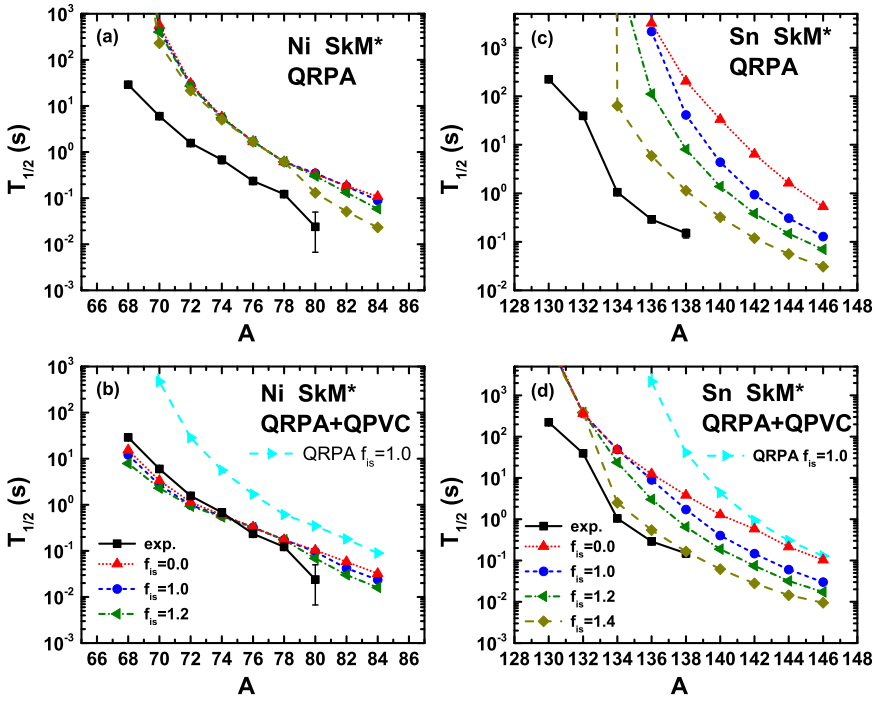

Fig. 5. (Colour online.) The β-decay half-lives of Ni isotopes [panel (a) and (b)] and Sn isotopes [panel (c) and (d)], calculated either by QRPA [panel (a) and (c)] or QRPA+QPVC model [panel (b) and (d)]. The Skyrme interaction SkM* is employed, together with the IV pairing force with $f_{iv} = 1.0$ and with IS pairing forces characterised by different strengths. The results are compared with experimental data from [52].

QRPA+QPVC level. The effects are particularly pronounced for Sn isotopes, where the influence of isoscalar pairing is very significant right after the magic nucleus ^{132}Sn, at variance with the case of IV pairing. The case of ^{134}Sn is analysed in detail in Fig. 6.

One can refer to the single-particle spectra shown in Fig. 3 in the following discussion. Before the $N = 50$ or $N = 82$ shell is filled, the transitions that contribute to the lowest GT energy state are mainly the back spin flip transitions, $\nu 2p_{1/2} \rightarrow \pi 2p_{3/2}$ (for Ni) and $\nu 2d_{3/2} \rightarrow \pi 2d_{5/2}$ (for Sn). For these configurations involving low angular momentum states, the IS pairing matrix elements are small. Furthermore, in the QRPA calculation these matrix elements are multiplied by the factor $u_\pi u_\pi u_\nu u_\nu + v_\pi v_\pi v_\nu v_\nu = u_\nu^2$ factors (the initial nucleus is closed shell in protons, so that $v_{\pi 2p_{3/2}}, v_{\pi 2d_{5/2}} = 0$) which is also small. Thus, IS pairing does not

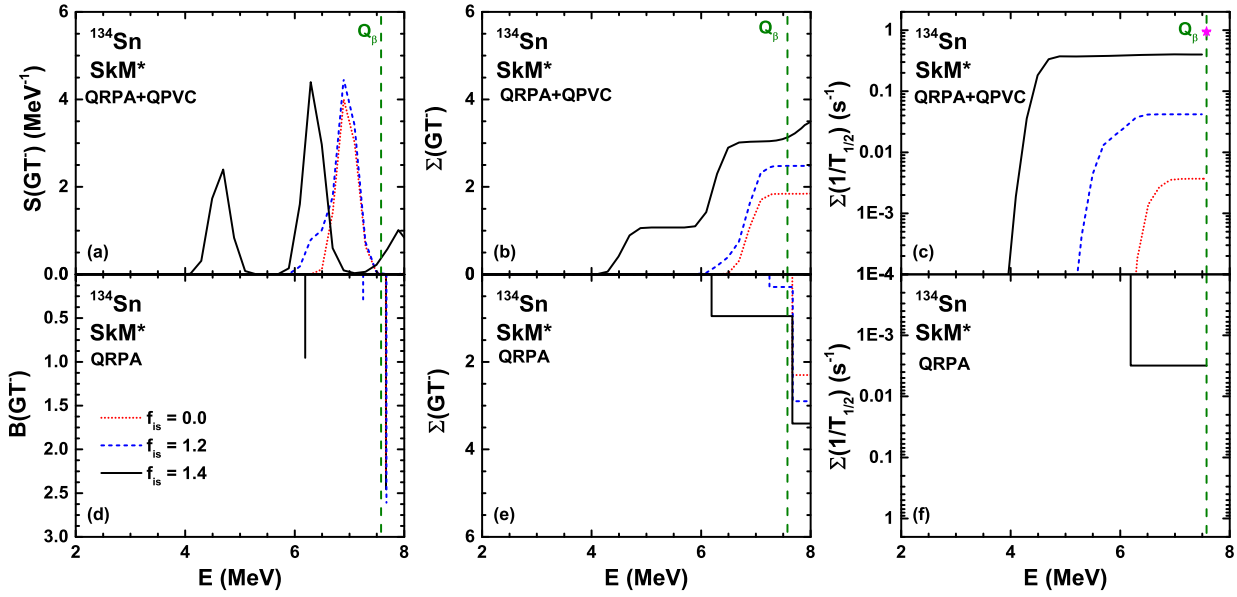

Fig. 6. (Colour online.) The same as Fig. 4, but for ^{134}Sn calculated with different isoscalar pairing strengths.

play a significant role for nuclei with neutron number smaller than $N = 50$ and $N = 82$ shell, as already found in refs. [16,26]. On the other hand, after crossing the $N = 50$ and $N = 82$ shell closures, the transitions $\nu 1g_{7/2} \rightarrow \pi 1g_{9/2}$ (for Ni) and $\nu 1h_{9/2} \rightarrow \pi 1h_{11/2}$ (for Sn) start to contribute in an important way, because these configurations are associated with large attractive IS pairing matrix elements and large u_v^2 factors. For nuclei just above the shell closure like $^{80-84}$Ni and $^{134-138}$Sn, where the $\nu 1g_{7/2}$ ($\nu 1h_{11/2}$) orbital is barely occupied, at $f_{is} = 0$, the configuration of $\nu 1g_{7/2} \rightarrow \pi 1g_{9/2}$ (for Ni) or $\nu 1h_{9/2} \rightarrow \pi 1h_{11/2}$ (for Sn) has higher unperturbed energy than that of $\nu 2p_{1/2} \rightarrow \pi 2p_{3/2}$ (for Ni) and $\nu 2d_{3/2} \rightarrow \pi 2d_{5/2}$ (for Sn), and hence the lowest GT state is dominated by $\nu 2p_{1/2} \rightarrow \pi 2p_{3/2}$ (for Ni) and $\nu 2d_{3/2} \rightarrow \pi 2d_{5/2}$ (for Sn). With the inclusion of IS pairing, the configuration of $\nu 1g_{7/2} \rightarrow \pi 1g_{9/2}$ (for Ni) or $\nu 1h_{9/2} \rightarrow \pi 1h_{11/2}$ (for Sn) is pushed to lower energy, and attracts strength from other transitions. This produces a low-lying, collective state in the QRPA calculation, which is shown in Fig. 6(d) in the case of ^{134}Sn. The energy of this state is very sensitive to the value of f_{is}. For nuclei that are further away from the $N = 50$ and $N = 82$ shell closures, like $^{140-146}$Sn, the $\nu 1g_{7/2} \rightarrow \pi 1g_{9/2}$ (for Ni) or $\nu 1h_{9/2} \rightarrow \pi 1h_{11/2}$ (for Sn) transition already dominates the lowest GT state in the $f_{is} = 0$ case; nonetheless, the inclusion of IS pairing further lowers the GT energy due to the attractive character of the matrix elements involving these configurations.

At the QPVC level, the effect of IS pairing is similar to that found in QRPA, because the isoscalar pairing does not enter the calculation of the self-energies.

For the Ni isotopes we have considered, since the effect of isoscalar pairing is small, the inclusion of QPVC is crucial to reproduce the experimental half-lives. In the case of Sn isotopes, isoscalar pairing and QPVC cooperate and improve the agreement with experimental data, as compared to the QRPA result with $f_{is} = 0$ (see Fig. 5(d)). The experimental half-lives are well reproduced in the QRPA+QPVC model with isoscalar pairing strength $f = 1.4$. This value is in good agreement with that reported in Ref. [47].

In Fig. 6, the GT strength distributions (with respect to the daughter nucleus), the cumulative sums of the strengths, and the cumulative sums of $1/T_{1/2}$ are shown in the case of ^{134}Sn, in a similar way as in Fig. 4 but for various values of the isoscalar pairing strength. In QRPA, the excitation energy of the main low-lying peak is almost unchanged by increasing f_{is}, whereas at the QPVC level it is not changed going from $f_{is} = 0$ to $f_{is} = 1.2$ but it moves downwards going from $f_{is} = 1.2$ to $f_{is} = 1.4$. Both in QRPA and QPVC, starting from $f_{is} = 1.2$ a new state located at lower energy appears, and with the IS pairing strength further increasing to $f_{is} = 1.4$ this lower state shifts downwards in energy and increases in strength. This new state is composed mainly by the transition $\nu 1h_{9/2} \rightarrow \pi 1h_{11/2}$ which is very sensitive to the attractive character of IS pairing. From QRPA to QPVC, the GT energy is shifted downwards by around 0.6 MeV in the case of $f = 0$ and $f = 1.2$, while the shift is around 1.5 MeV in the case of $f = 1.4$. With the increase of IS pairing strength, the cumulative sum of strength within the Q_β values is increased too. Due to the downward shift in GT energy, the QRPA model leads to a finite life time for $f_{is} = 1.4$, but it still greatly overestimates the half-life. With the inclusion of QPVC, since the GT energy is further reduced, the theoretical model can provide a good reproduction of the experimental half-life for $f_{is} = 1.4$.

4. Conclusions

In summary, we have calculated the half-lives of a chain of Ni and Sn isotopes around the closed shell nuclei ^{78}Ni and ^{132}Sn, in the framework of the self-consistent QRPA+QPVC model based on Skyrme density functional SkM*, which has been shown to lead to a good agreement with experiment for half-lives of magic nuclei [44] and GT transitions of both magic [42] and superfluid nuclei [45]. We have investigated in detail the effects of IV pairing and IS pairing, both at QRPA and QRPA+QPVC level. It is found that IV pairing mainly plays a role for nuclei before closed shell, and it increases the half-lives. However, this effect is greatly reduced when QPVC is taken into account, as compared to QRPA. On the contrary, IS pairing mainly plays a role for nuclei after closed shell, and it decreases the half-lives. The effect of IS pairing is similar at QRPA and QRPA+QPVC level. In our calculations, IS pairing plays an important role in the case of Sn isotopes beyond ^{132}Sn, where it reinforces the action of QPVC in reducing the half-lives; good agreement with experiment is found assuming a value of the isoscalar pairing strength $f_{is} = 1.4$. Most of the Ni isotopes we have considered lie before ^{78}Ni, so that the effect of isoscalar pairing is small; also in this case good agreement with experiment is

found once the QPVC is included. In the present work, only GT transition is considered in the half-life calculation. The study on the role of forbidden transitions in the framework of QRPA+QPVC is envisaged.

Acknowledgements

This work was partly supported by the National Natural Science Foundation of China under Grant Nos. 11305161, 11205004 and the Natural Science Foundation of Anhui Province under Grant No. 1708085QA10. G.C. and E.V. acknowledge funding from the European Union Horizon 2020 research and innovation program under Grant Agreement No. 654002.

References

[1] E.M. Burbidge, G.R. Burbidge, W.A. Fowler, F. Hoyle, Rev. Mod. Phys. 29 (1957) 547.
[2] Y.-Z. Qian, G.J. Wasserburg, Phys. Rep. 442 (2007) 237.
[3] K. Langanke, G. Martínez-Pinedo, Rev. Mod. Phys. 75 (2003) 819.
[4] C.S. Wu, E. Ambler, R.W. Hayward, D.D. Hoppes, R.P. Hudson, Phys. Rev. 105 (1957) 1413.
[5] H. Liang, N. Van Giai, J. Meng, Phys. Rev. C 79 (2009) 064316.
[6] I.S. Towner, J.C. Hardy, Rep. Prog. Phys. 73 (2010) 046301.
[7] S. Nishimura, Z. Li, H. Watanabe, K. Yoshinaga, T. Sumikama, T. Tachibana, K. Yamaguchi, M. Kurata-Nishimura, G. Lorusso, Y. Miyashita, et al., Phys. Rev. Lett. 106 (2011) 052502.
[8] Z.Y. Xu, S. Nishimura, G. Lorusso, F. Browne, P. Doornenbal, G. Gey, H.-S. Jung, Z. Li, M. Niikura, P.-A. Söderström, et al., Phys. Rev. Lett. 113 (2014) 032505.
[9] G. Lorusso, S. Nishimura, Z.Y. Xu, A. Jungclaus, Y. Shimizu, G.S. Simpson, P.-A. Söderström, H. Watanabe, F. Browne, P. Doornenbal, et al., Phys. Rev. Lett. 114 (2015) 192501.
[10] J. Wu, S. Nishimura, G. Lorusso, P. Möller, E. Ideguchi, P.-H. Regan, G.S. Simpson, P.-A. Söderström, P.M. Walker, H. Watanabe, et al., Phys. Rev. Lett. 118 (2017) 072701.
[11] I. Borzov, Nucl. Phys. A 777 (2006) 645.
[12] D.-L. Fang, B.A. Brown, T. Suzuki, Phys. Rev. C 88 (2013) 034304.
[13] H. Homma, E. Bender, M. Hirsch, K. Muto, H.V. Klapdor-Kleingrothaus, T. Oda, Phys. Rev. C 54 (1996) 2972.
[14] P. Möller, J.R. Nix, K.L. Kratz, At. Data Nucl. Data Tables 66 (1997) 131.
[15] I.N. Borzov, S. Goriely, Phys. Rev. C 62 (2000) 035501.
[16] J. Engel, M. Bender, J. Dobaczewski, W. Nazarewicz, R. Surman, Phys. Rev. C 60 (1999) 014302.
[17] P. Sarriguren, E. Moya de Guerra, A. Escuderos, Phys. Rev. C 64 (2001) 064306.
[18] K. Yoshida, Prog. Theor. Exp. Phys. 113D02 (2013).
[19] M. Martini, S. Péru, S. Goriely, Phys. Rev. C 89 (2014) 044306.
[20] P. Sarriguren, Phys. Rev. C 91 (2015) 044304.
[21] M.T. Mustonen, J. Engel, Phys. Rev. C 93 (2016) 014304.
[22] J. Meng, H. Toki, S. Zhou, S. Zhang, W. Long, L. Geng, Prog. Part. Nucl. Phys. 57 (2006) 470.
[23] H.Z. Liang, N. Van Giai, J. Meng, Phys. Rev. Lett. 101 (2008) 122502.
[24] N. Paar, T. Nikšić, D. Vretenar, P. Ring, Phys. Rev. C 69 (2004) 054303.
[25] Z.M. Niu, Y.F. Niu, H.Z. Liang, W.H. Long, J. Meng, Phys. Rev. C 95 (2017) 044301.
[26] T. Nikšić, T. Marketin, D. Vretenar, N. Paar, P. Ring, Phys. Rev. C 71 (2005) 014308.
[27] T. Marketin, D. Vretenar, P. Ring, Phys. Rev. C 75 (2007) 024304.
[28] T. Marketin, L. Huther, G. Martínez-Pinedo, Phys. Rev. C 93 (2016) 025805.
[29] Z.M. Niu, Y.F. Niu, H.Z. Liang, W.H. Long, T. Nikšić, D. Vretenar, J. Meng, Phys. Lett. B 723 (2013) 172.
[30] Z.M. Niu, Y.F. Niu, Q. Liu, H.Z. Liang, J.Y. Guo, Phys. Rev. C 87 (2013) 051303.
[31] Z.Y. Wang, Y.F. Niu, Z.M. Niu, J.Y. Guo, J. Phys. G, Nucl. Part. Phys. 43 (2016) 045108.
[32] F. Minato, C.L. Bai, Phys. Rev. Lett. 110 (2013) 122501.
[33] A.P. Severyukhin, V.V. Voronov, I.N. Borzov, N.N. Arsenyev, N. Van Giai, Phys. Rev. C 90 (2014) 044320.
[34] V.A. Kuzmin, V.G. Soloviev, J. Phys. G 10 (1984) 1507.
[35] S. Drożdż, S. Nishizaki, J. Speth, J. Wambach, Phys. Rep. 197 (1990) 1.
[36] N. Dinh Dang, A. Arima, T. Suzuki, S. Yamaji, Phys. Rev. Lett. 79 (1997) 1638.
[37] D. Gambacurta, M. Grasso, F. Catara, Phys. Rev. C 84 (2011) 034301.
[38] D. Gambacurta, M. Grasso, V. De Donno, G. Co', F. Catara, Phys. Rev. C 86 (2012) 021304.
[39] G.F. Bertsch, P.F. Bortignon, R.A. Broglia, Rev. Mod. Phys. 55 (1983) 287.
[40] E. Litvinova, B.A. Brown, D.-L. Fang, T. Marketin, R.G.T. Zegers, Phys. Lett. B 730 (2014) 307.
[41] T. Marketin, E. Litvinova, D. Vretenar, P. Ring, Phys. Lett. B 706 (2012) 477.
[42] Y.F. Niu, G. Colò, M. Brenna, P.F. Bortignon, J. Meng, Phys. Rev. C 85 (2012) 034314.
[43] Y.F. Niu, G. Colò, E. Vigezzi, Phys. Rev. C 90 (2014) 054328.
[44] Y.F. Niu, Z.M. Niu, G. Colò, E. Vigezzi, Phys. Rev. Lett. 114 (2015) 142501.
[45] Y.F. Niu, G. Colò, E. Vigezzi, C.L. Bai, H. Sagawa, Phys. Rev. C 94 (2016) 064328.
[46] C. Robin, E. Litvinova, Eur. Phys. J. A 52 (2016) 205.
[47] H. Sagawa, C.L. Bai, G. Colò, Phys. Scr. 91 (2016) 083011.
[48] C.L. Bai, H. Sagawa, G. Colò, Y. Fujita, H.Q. Zhang, X.Z. Zhang, F.R. Xu, Phys. Rev. C 90 (2014) 054335.
[49] C. Mahaux, P.F. Bortignon, R.A. Broglia, C.H. Dasso, Phys. Rep. 120 (1985) 1.
[50] A. de Shalit, H. Feshbach, Theoretical Nuclear Physics, vol. 1. Nuclear Structure, J. Wiley and Sons, New York, 1974.
[51] A. Bohr, B.R. Mottelson, Nuclear Structure, vol. II, Benjamin, New York, 1975.
[52] G. Audi, F.G. Kondev, M. Wang, W.J. Huang, S. Naimi, Chin. Phys. C 41 (2017) 030001.
[53] http://www.nndc.bnl.gov.